

CloudSat Project

A NASA Earth System Science Pathfinder Mission

Level 2B Radar-only Cloud Water Content (2B-CWC-RO) Process Description Document

Version: 5.1

Date: 21 October 2007

Questions concerning the document and proposed changes should be addressed to

Richard Austin

austin@atmos.colostate.edu

+1 970 491 8587

Contents

1	Introduction	3
2	Algorithm Theoretical Basis—Liquid Water Content	4
2.1	Forward Model and Measurements	4
2.1.1	Physics of the Forward Model	4
2.1.2	Departures From the Lognormal Distribution	6
2.1.3	Mixed phase and multi-layered clouds	6
2.2	Retrieval Algorithm	7
2.2.1	State and Measurement Vectors	7
2.2.2	Forward Model and Parameters	8
2.2.3	A Priori Data and Covariance	9
2.2.4	Convergence and Quality Control	10
3	Algorithm Theoretical Basis—Ice Water Content	11
3.1	Forward Model and Measurements	11
3.1.1	Physics of the Forward Model	11
3.1.2	Algorithm refinements: correction for Lorenz-Mie effects	12
3.1.3	Further possible algorithm refinements: correction for density effects	13
3.1.4	Departures from the Lognormal Distribution	14
3.1.5	Mixed phase and multi-layered clouds	14
3.2	Retrieval Algorithm	14
3.2.1	State and Measurement Vectors	14
3.2.2	Forward Model and Parameters	15
3.2.3	A Priori Data and Covariance	15
3.2.4	Convergence and Quality Control	16
4	Algorithm Theoretical Basis—Cloud Water Content	17
5	Algorithm Inputs	19
5.1	CloudSat	19
5.1.1	CloudSat 2B-GEOPROF Data	19
5.1.2	CloudSat 2B-CLDCLASS Data	19
5.2	Ancillary (Non-CloudSat)	19
5.2.1	CloudSat ECMWF-AUX Data	19
6	Algorithm Summary	20
7	Data Product Output Format	23
8	Changes since version 5.0	23

1 Introduction

The CloudSat Radar-Only Cloud Water Content Product (2B-CWC-RO) contains retrieved estimates of cloud liquid and ice water content, effective radius, and related quantities for each radar profile measured by the Cloud Profiling Radar on CloudSat. Retrievals are performed separately for the liquid and ice phases; the two sets of results are then combined in a simple way to obtain a composite profile that is consistent with the input measurements.

This radar-only (RO) product uses measured radar reflectivity factor as the sole input from remote sensing instruments. A similar CloudSat standard data product, 2B-CWC-RVOD, uses estimates of visible optical depth (from the CloudSat 2B-TAU product) together with the radar measurements to more tightly constrain the retrievals, which should result in more accurate results. However, retrievals of visible optical depth are difficult or impossible in many cases, due to the complexity of the targets and the simplifying assumptions made necessary by the data volumes associated with an operational satellite. Therefore, the CloudSat retrievals are produced in both radar-only (RO) and radar-visible optical depth (RVOD) versions, allowing the user to work with the generally available RO data, which are supplemented by the RVOD solutions where possible. The 2B-CWC-RVOD product should be released a few months after the RO product.

The CWC algorithm creates a composite profile from separate ice and liquid water retrievals. Both of these retrievals assume that the radar profile is due to a single phase of water, that is, that the entire profile consists of either liquid or ice, but not both. The resulting separate liquid and ice profiles are then combined using a simple scheme based on temperature as reported by an ECMWF model. While the combination algorithm results in a mixture of ice and liquid phases over that part of the vertical profile that has the proper temperature range, the user should be aware that the retrieval does not attempt to retrieve mixed-phase cloud properties directly. Improvements are in the planning stages to better handle the retrieval of mixed-phase cloud.

This document describes the algorithms that have been implemented in Release 4 (R04) of the 2B-CWC-RO product (algorithm version 5.1). For each radar profile, the algorithms will

- Examine the cloud mask in 2B-GEOPROF to determine which bins in the column contain cloud,
- Examine the 2B-CLDCLASS product to determine if any cloudy bins have an undetermined or invalid cloud type (indicating a problematic profile),
- Assign *a priori* values to the liquid and ice particle size distribution parameters in each cloudy bin based on climatology, temperature, or other criteria,
- Using the *a priori* values and radar measurements from 2B-GEOPROF, retrieve liquid and ice particle size distribution parameters for each cloudy bin. Derive effective radius, water content, and related quantities from the retrieved size distributions for both liquid and ice phases, together with associated uncertainties,
- Create a composite profile by using the retrieved ice properties at temperatures colder than -20°C , the retrieved liquid properties at temperatures warmer than 0°C , and a linear combination of the two in intermediate temperatures,
- For each of these estimates, calculate uncertainties and covariance matrices.

2 Algorithm Theoretical Basis—Liquid Water Content

The liquid cloud retrieval algorithm is a modification of the method described in Austin and Stephens (200X). [A previous version of the algorithm is described in Austin and Stephens (2001).] Condensed versions of the descriptions of the forward model and retrieval formulation are given here and in the following section, together with a description of modifications specific to the operational CloudSat algorithm.

2.1 Forward Model and Measurements

The retrieval uses active remote sensing data together with *a priori* data to estimate the parameters of the particle size distribution in each bin containing cloud. Radar measurements provide a vertical profile of cloud backscatter; the measured backscatter value and a cloud mask (indicating the likelihood that a particular radar bin contains cloud) are obtained from 2B-GEOPROF.

2.1.1 Physics of the Forward Model

The forward model developed for the retrieval assumes a lognormal size distribution of cloud droplets:

$$N(r) = \frac{N_T}{\sqrt{2\pi}\sigma_{\log}r} \exp\left[\frac{-\ln^2(r/r_g)}{2\sigma_{\log}^2}\right], \quad (1)$$

where N_T is the droplet number density, r is the droplet radius, and r_g , σ_{\log} , and σ_g are defined by

$$\begin{aligned} \ln r_g &= \overline{\ln r}, \\ \sigma_{\log} &= \ln \sigma_g, \\ \sigma_g^2 &= \overline{(\ln r - \ln r_g)^2}, \end{aligned}$$

where r_g is the geometric mean radius, σ_{\log} is the distribution width parameter, σ_g is the geometric standard deviation, \ln indicates the natural (base e) logarithm, and the overbar indicates the arithmetic mean. The distribution in (1) is fully specified by three parameters: N_T , σ_{\log} , and r_g . The liquid water content LWC and the effective radius r_e are defined in terms of moments of the size distribution:

$$\text{LWC} = \int_0^\infty \rho_w N(r) \frac{4}{3} \pi r^3 dr, \quad (2)$$

$$r_e = \frac{\int_0^\infty N(r) r^3 dr}{\int_0^\infty N(r) r^2 dr}, \quad (3)$$

where ρ_w is the density of water.

For clouds having negligible drizzle or precipitation, cloud droplets are sufficiently small to be modeled as Rayleigh scatterers at the CloudSat radar wavelength and sufficiently large that their extinction efficiency approaches 2 for visible wavelengths. These assumptions yield the following definitions of radar reflectivity factor Z and visible extinction coefficient σ_{ext} :

$$Z = 64 \int_0^\infty N(r) r^6 dr, \quad (4)$$

$$\sigma_{\text{ext}} = 2 \int_0^{\infty} N(r) \pi r^2 dr. \quad (5)$$

Using (1) for the size distribution in (2) through (5) gives the following equations for the various cloud properties:

$$\text{LWC} = \frac{4\pi}{3} N_T \rho_w r_g^3 \exp\left(\frac{9}{2} \sigma_{\log}^2\right), \quad (6)$$

$$r_e = r_g \exp\left(\frac{5}{2} \sigma_{\log}^2\right), \quad (7)$$

$$Z = 64 N_T r_g^6 \exp(18 \sigma_{\log}^2), \quad (8)$$

$$\sigma_{\text{ext}} = 2\pi N_T r_g^2 \exp(2 \sigma_{\log}^2). \quad (9)$$

All of these properties are functions of position in the cloud column; we can therefore write $\text{LWC}(z)$, $r_e(z)$, $Z(z)$, and $\sigma_{\text{ext}}(z)$.

The visible optical depth τ is calculated by integrating the visible extinction coefficient through the cloud column:

$$\tau = \int_{z_{\text{base}}}^{z_{\text{top}}} \sigma_{\text{ext}}(z) dz, \quad (10)$$

where z_{base} and z_{top} are the cloud base and top, respectively. Equations (6) through (10) express the intrinsic properties of the cloud as functions of the parameters of the assumed drop size distribution; they form the basis of the retrieval. LWC and r_e are the quantities we seek to retrieve, and values of Z are related to our measurements. We may also specify LWP, the columnar liquid water content or liquid water path,

$$\text{LWP} = \int_{z_{\text{base}}}^{z_{\text{top}}} \text{LWC}(z) dz. \quad (11)$$

The scattered energy received by the radar from particles at a given range will be attenuated in both directions by cloud particles between that range and the radar receiver. (It will also experience gaseous attenuation, primarily by water vapor; this attenuation is provided as a separate variable in the 2B-GEOPROF product and is therefore not considered here.) The measured reflectivity factor Z' will be reduced from the intrinsic reflectivity factor Z according to the following expression:

$$Z'(z) = Z(z) \exp\left[-2 \int_{\text{path}} \sigma_{\text{abs}}(z') dz'\right], \quad (12)$$

where the path integral is over the portion of the cloud between z and the radar. The absorption coefficient at the radar frequency σ_{abs} is given by

$$\sigma_{\text{abs}}(z) = \int_0^{\infty} N(r, z) C_{\text{abs}}(r) dr, \quad (13)$$

where $N(r, z)$ is the particle size distribution at z and C_{abs} is the absorption cross section as a function of particle radius r . (Scattering effects are much smaller than absorption effects at the radar wavelength, so we approximate the attenuation as being purely due to absorption.)

Assuming the cloud droplets are sufficiently small to be modeled as spherical droplets, we may use Mie theory to obtain an expression for C_{abs} :

$$C_{\text{abs}} = \frac{8\pi^2 r^3}{\lambda} \text{Im}\{-K\}, \quad (14)$$

where λ is the radar wavelength and K is given by

$$K = \frac{m^2 - 1}{m^2 + 2}, \quad (15)$$

where m is the complex index of refraction of the droplet material (water) at the radar frequency and ambient temperature. Using the lognormal distribution in (1), the absorption coefficient in (13) becomes

$$\sigma_{\text{abs}} = \frac{8\pi^2 N_T}{\lambda} \text{Im}\{-K\} r_g^3 \exp\left(\frac{9}{2}\sigma_{\log}^2\right), \quad (16)$$

where the z dependence is suppressed for clarity.

Assuming that a lognormal distribution is appropriate, the cloud microphysics are fully described by specification of the three lognormal distribution parameters $N_T(z)$, $\sigma_{\log}(z)$, and $r_g(z)$. Liquid water content and effective radius may then be obtained through (6) and (7). Because the measured data are limited to a single radar reflectivity factor Z' for each radar resolution bin, we rely on *a priori* data to constrain the retrieval where the measurements cannot, allowing the retrieved solution to be consistent with the measurements without imposing fixed values of (e.g.) particle number concentration through the cloud column. The optimal estimation technique employed in this retrieval is described in section 2.2.

2.1.2 Departures From the Lognormal Distribution

The retrieval assumes a lognormal distribution of liquid cloud droplets, as given in (1). Departures from this distribution will degrade the accuracy of the retrieval. One source of departure from this analytic distribution is the presence of drizzle or rain within the cloud. Detection criteria for the presence of drizzle or rain are under development. (The current procedure identifies drizzle or precipitation for any case where $Z' \geq -15$ dBZ.) Drizzle/precipitation is indicated in the output by setting a flag in the status variable, but the algorithm is still run as normal, producing output values (unless the solution diverges). The flag serves as an indicator that the solution is likely unreliable due to a violation of the lognormal distribution assumption. In practice, the presence of any significant precipitation causes the retrieval to fail to converge, resulting in an error condition. Retrieval of cloud properties in the presence of precipitation is a difficult problem due to the sensitivity of the radar to precipitation-sized particles. Better handling of this case is a high priority for future development of this product.

2.1.3 Mixed phase and multi-layered clouds

The liquid water content retrieval algorithm assumes that the entire cloud column is composed of liquid water droplets. (The retrievals used in 2B-CWC-RO consider only one phase of water at a time.) Because we have no independent means of determining the particle phase in a given radar bin, a simple partition scheme is employed to create a composite ice/liquid profile, discarding the retrieved liquid properties in portions of the profile deemed to consist purely of ice. The partition scheme is described in section 4.

2.2 Retrieval Algorithm

The retrieval uses an approach described by Rodgers (1976, 1990, 2000) and Marks and Rodgers (1993), where a vector of measured quantities \mathbf{y} (here, radar reflectivities) is related to a state vector of unknowns \mathbf{x} (geometric mean radii, number density, and distribution width parameter) by the forward model \mathbf{F} :

$$\mathbf{y} = \mathbf{F}(\mathbf{x}) + \epsilon_{\mathbf{y}}, \quad (17)$$

where $\epsilon_{\mathbf{y}}$ represents measurement errors. Rodgers (1976) described an optimal-estimation technique in which *a priori* profiles are used as virtual measurements, serving as a constraint on the retrieval. An *a priori* profile \mathbf{x}_a is specified based on likely or statistical values of the state vector elements, together with an *a priori* covariance matrix \mathbf{S}_a representing the variability or uncertainty of this profile and the covariance between various profile elements.

The retrieval algorithm obtains the optimal solution by minimizing a cost function Φ that represents a weighted sum of the measurement vector-forward model difference and the state vector-*a priori* difference:

$$\Phi = (\hat{\mathbf{x}} - \mathbf{x}_a)^T \mathbf{S}_a^{-1} (\hat{\mathbf{x}} - \mathbf{x}_a) + [\mathbf{y} - \mathbf{F}(\hat{\mathbf{x}})]^T \mathbf{S}_y^{-1} [\mathbf{y} - \mathbf{F}(\hat{\mathbf{x}})]. \quad (18)$$

The solution is obtained by iteration using successive estimates of the \mathbf{x} vector and the \mathbf{K} matrix ($\mathbf{K} = \partial\mathbf{F}/\partial\mathbf{x}$). These quantities are also used to provide information on convergence, the quality of the solution, and the amounts and sources of retrieval uncertainty. The various input and output quantities are described here; see Austin and Stephens (200X) for a more detailed description.

2.2.1 State and Measurement Vectors

The state vector \mathbf{x} is the vector of unknown cloud parameters to be retrieved. For a cloud reflectivity profile consisting of p cloudy bins, the state vector will have $n = 3p$ elements:

$$\mathbf{x} = \begin{bmatrix} r_g(z_1) \\ \vdots \\ r_g(z_p) \\ N_T(z_1) \\ \vdots \\ N_T(z_p) \\ \sigma_{\log}(z_1) \\ \vdots \\ \sigma_{\log}(z_p) \end{bmatrix}, \quad (19)$$

where $r_g(z_i)$, $N_T(z_i)$, and $\sigma_{\log}(z_i)$ are the geometric mean radius, droplet number concentration, and distribution width parameter for height z_i (we shall often write these as r_{g_i} , etc.). Here z_1 is the height of the radar resolution bin at cloud base; z_p is at the top of the cloud profile. Units are selected to keep the numerical values within similar orders of magnitude: μm for r_g and cm^{-3} for N_T (σ_{\log} is dimensionless).

The RO measurement vector \mathbf{y} is composed of $m = p$ elements for a cloud profile of p cloudy bins:

$$\mathbf{y} = \begin{bmatrix} Z'_{\text{dB}}(z_1) \\ \vdots \\ Z'_{\text{dB}}(z_p) \end{bmatrix}, \quad (20)$$

where $Z'_{\text{dB}}(z_i)$ is the measured radar reflectivity factor for height z_i (often written as Z'_{dB_i}). Reflectivity factor Z is specified in units of $\text{mm}^6 \text{m}^{-3}$. To reduce the large dynamic range of the reflectivity variable and to make the model more linear, Z has been converted to a logarithmic variable Z_{dB} by the transform $Z_{\text{dB}} = 10 \log Z$, where Z_{dB} has units of dBZ and \log indicates the base 10 logarithm.

The measurement error covariance matrix \mathbf{S}_ϵ gives a measure of the uncertainties in the measurement vector and of correlations between the errors of the individual elements. In the present retrieval, it is assumed that the elements of \mathbf{y} have independent errors given as follows:

$$\mathbf{S}_\epsilon = \begin{bmatrix} \sigma_{Z'_{\text{dB}_1}}^2 & 0 & \cdots & 0 \\ 0 & \ddots & 0 & \vdots \\ \vdots & 0 & \ddots & 0 \\ 0 & \cdots & 0 & \sigma_{Z'_{\text{dB}_p}}^2 \end{bmatrix}, \quad (21)$$

where $\sigma_{Z'_{\text{dB}_i}}$ is the standard deviation of the measured radar reflectivity factor in dBZ (i.e., the uncertainty in the measured radar reflectivity values from whatever source [noise, calibration error, etc.], usually a fixed number for a given radar).

2.2.2 Forward Model and Parameters

The forward model $\mathbf{F}(\mathbf{x})$ relates the state vector \mathbf{x} to the measurement vector \mathbf{y} . \mathbf{F} therefore has the same dimension as \mathbf{y} :

$$\mathbf{F}(\mathbf{x}) = \begin{bmatrix} Z'_{\text{dB}_{\text{FM}}}(z_1) \\ \vdots \\ Z'_{\text{dB}_{\text{FM}}}(z_p) \end{bmatrix}, \quad (22)$$

where the individual elements are given by the following expressions:

$$\begin{aligned} Z'_{\text{dB}_{\text{FM}}}(z_i) = & 10 \log \left\{ 64 N_T r_{g_i}^6 \exp(18 \sigma_{\log}^2) \right. \\ & \times \exp \left[\frac{-16 \pi^2 N_T}{\lambda} \text{Im}\{-K\} \right. \\ & \left. \left. \times \exp \left(\frac{9}{2} \sigma_{\log}^2 \right) \Delta z \sum_{j=i+1}^p r_{g_j}^3 \right] \right\}, \quad i = 1, \dots, p-1 \end{aligned} \quad (23)$$

$$Z'_{\text{dB}_{\text{FM}}}(z_i) = 10 \log \left[64 N_T r_{g_i}^6 \exp(18 \sigma_{\log}^2) \right], \quad i = p \quad (24)$$

(The symbol Δz represents the thickness of a radar range bin.) The subscript FM is a reminder that these quantities are calculated from elements of \mathbf{x} according to the forward model equations (23) and (24), as opposed to the elements of the \mathbf{y} vector, which are measured quantities. The form of (23) and (24) assumes that the radar is above the cloud looking down; again, z_1 is the lowest bin in the cloud and z_p is the highest.

2.2.3 A Priori Data and Covariance

A priori data for the retrieval are selected based on collections of microphysical measurements of related cloud types. Reference values for each of these categories are obtained from a database of cloud microphysical parameters (e.g., Miles et al. 2000). The selected values for each radar profile are included in the product output. The *a priori* vector \mathbf{x}_a is specified as follows:

$$\mathbf{x}_a = \begin{bmatrix} r_{ga}(z_1) \\ \vdots \\ r_{ga}(z_p) \\ N_{Ta}(z_1) \\ \vdots \\ N_{Ta}(z_p) \\ \sigma_{\log_a}(z_1) \\ \vdots \\ \sigma_{\log_a}(z_p) \end{bmatrix}. \quad (25)$$

We also specify an *a priori* error covariance matrix \mathbf{S}_a :

$$\mathbf{S}_a = \begin{bmatrix} \sigma_{r_{ga_1}}^2 & 0 & \cdots & 0 & \cdots & 0 & 0 & \cdots & 0 \\ 0 & \ddots & 0 & \vdots & \vdots & \vdots & \vdots & \vdots & \vdots \\ \vdots & 0 & \sigma_{r_{ga_p}}^2 & 0 & \cdots & 0 & 0 & \cdots & 0 \\ 0 & \cdots & 0 & \sigma_{N_{Ta_1}}^2 & 0 & \vdots & \vdots & \vdots & \vdots \\ \vdots & \cdots & \vdots & 0 & \ddots & 0 & \vdots & \vdots & \vdots \\ 0 & \cdots & 0 & \cdots & 0 & \sigma_{N_{Ta_p}}^2 & 0 & \vdots & \vdots \\ 0 & \cdots & 0 & \cdots & \cdots & 0 & \sigma_{\sigma_{\log_a_1}}^2 & 0 & \vdots \\ \vdots & \cdots & \vdots & \cdots & \cdots & \cdots & 0 & \ddots & 0 \\ 0 & \cdots & 0 & \cdots & \cdots & \cdots & \cdots & 0 & \sigma_{\sigma_{\log_a_p}}^2 \end{bmatrix}. \quad (26)$$

Adjustment of the *a priori* parameters \mathbf{x}_a and uncertainties \mathbf{S}_a in future versions may allow customization of the retrieval for different cloud types, generation regimes (e.g., continental or maritime), and geographic areas (tropical, midlatitude, etc.).

2.2.4 Convergence and Quality Control

The state vector $\hat{\mathbf{x}}$ is obtained by iteration. The *a priori* values \mathbf{x}_a are used as the initial value of $\hat{\mathbf{x}}$. Convergence of the solution is determined using a test with the following form:

$$\Delta\hat{\mathbf{x}}^T \mathbf{S}_x^{-1} \Delta\hat{\mathbf{x}} \ll n, \quad (27)$$

where n is the dimension of the $\hat{\mathbf{x}}$ vector, i.e. the number of cloudy radar bins times three. The error covariance matrix \mathbf{S}_x of the retrieved state vector $\hat{\mathbf{x}}$ is given by

$$\mathbf{S}_x = (\mathbf{S}_a^{-1} + \mathbf{K}^T \mathbf{S}_y^{-1} \mathbf{K})^{-1}. \quad (28)$$

Elements of the \mathbf{S}_x matrix give the covariance between elements of the retrieved state vector $\hat{\mathbf{x}}$; diagonal elements of \mathbf{S}_x are variances in the elements of $\hat{\mathbf{x}}$ and give a measure of the uncertainty in the retrieval. For this retrieval, we specify the criterion for “much less than” in (27) such that

$$\Delta\hat{\mathbf{x}}^T \mathbf{S}_x^{-1} \Delta\hat{\mathbf{x}} < 0.01n. \quad (29)$$

After the iteration converges, we seek a test that shows the goodness of fit of the retrieved values to the measurements. Using the hypothesis that the fit to the measurements (including the *a priori* virtual measurements) is consistent with the measurement uncertainties (including the *a priori* uncertainties), Marks and Rodgers (1993) used the following χ^2 :

$$\chi^2 = [\mathbf{y} - \mathbf{F}(\hat{\mathbf{x}})]^T \mathbf{S}_y^{-1} [\mathbf{y} - \mathbf{F}(\hat{\mathbf{x}})] + (\mathbf{x}_a - \hat{\mathbf{x}})^T \mathbf{S}_a^{-1} (\mathbf{x}_a - \hat{\mathbf{x}}). \quad (30)$$

This quantity should follow a χ^2 distribution with m degrees of freedom (n parameters fitted to $m + n$ measurements, where n and m are the dimensions of the $\hat{\mathbf{x}}$ and \mathbf{y} vectors, respectively). Marks and Rodgers (1993) noted that a typical value of χ^2 for a “moderately good retrieval” is m .

As currently implemented, the retrieval rejects profiles where any element of the $\hat{\mathbf{x}}$ vector becomes negative during any iteration. (This is infrequent.) Profiles are also rejected if the measured reflectivity factor exceeds a specified maximum level (i.e., it is unphysical) or if the radar information is unavailable.

3 Algorithm Theoretical Basis—Ice Water Content

The retrieval algorithm is described in Austin et al. (200X); an earlier version is described by Benedetti et al. (2003). Condensed versions of the descriptions of the forward model and retrieval formulation are given here and in the following section, together with a description of modifications specific to the operational CloudSat algorithm.

3.1 Forward Model and Measurements

Like the liquid cloud retrieval, this retrieval uses active remote sensing data together with *a priori* data to estimate the parameters of the particle size distribution in each bin containing cloud. Radar measurements provide a vertical profile of cloud backscatter; the measured backscatter value and a cloud mask (indicating the likelihood that a particular radar bin contains cloud) are obtained from 2B-GEOPROF.

3.1.1 Physics of the Forward Model

The forward model developed for the retrieval assumes a lognormal size distribution of ice crystals:

$$N(D) = \frac{N_T}{\sqrt{2\pi}\sigma_{\log}D} \exp\left[\frac{-\ln^2(D/D_g)}{2\sigma_{\log}^2}\right], \quad (31)$$

where N_T is the ice particle number concentration, D is the diameter of an equivalent mass ice sphere, D_g is the geometric mean diameter, and σ_{\log} is the width parameter. The distribution in (31) is fully specified by three parameters: N_T , D_g , and σ_{\log} . The ice water content (IWC) and the effective radius r_e are defined in terms of moments of the size distribution:

$$\text{IWC} = \int_0^{\infty} \rho_i \frac{\pi}{6} N(D) D^3 dD \quad (32)$$

$$r_e = \frac{1}{2} \frac{\int_0^{\infty} N(D) D^3 dD}{\int_0^{\infty} N(D) D^2 dD}, \quad (33)$$

where ρ_i is the density of ice.

For thin ice clouds, the cloud ice particles are sufficiently small to be modeled as Rayleigh scatterers at the CloudSat radar wavelength and sufficiently large that their extinction efficiency approaches 2 for visible wavelengths. These assumptions yield the following definitions of radar reflectivity factor Z and visible extinction coefficient σ_{ext} :

$$Z_{\text{Ray}} = \int_0^{\infty} N(D) D^6 dD \quad (34)$$

$$\sigma_{\text{ext}} = 2 \int_0^{\infty} N(D) \frac{\pi}{4} D^2 dD \quad (35)$$

Using (31) for the size distribution in (32) through (35) gives the following equations for the various cloud properties:

$$\text{IWC} = \rho_i \frac{\pi}{6} N_T D_g^3 \exp\left(\frac{9}{2}\sigma_{\log}^2\right) 10^{-3} \quad (36)$$

$$r_e = \frac{1}{2} D_g \exp\left(\frac{5}{2} \sigma_{\log}^2\right) 10^3 \quad (37)$$

$$\sigma_{\text{ext}} = \frac{\pi}{2} N_T D_g^2 \exp(2\sigma_{\log}^2) 10^{-3} \quad (38)$$

$$Z_{\text{Ray}} = N_T D_g^6 \exp(18\sigma_{\log}^2), \quad (39)$$

All of these properties are functions of position in the cloud column; we can therefore write $\text{IWC}(z)$, $r_e(z)$, $\sigma_{\text{ext}}(z)$, and $Z_{\text{Ray}}(z)$.

The visible optical depth τ is calculated by integrating the visible extinction coefficient through the cloud column:

$$\tau = \int_{z_{\text{base}}}^{z_{\text{top}}} \sigma_{\text{ext}}(z) dz, \quad (40)$$

where z_{base} and z_{top} are the cloud base and top, respectively. Equations (36) through (40) express the intrinsic properties of the cloud as functions of the parameters of the assumed particle size distribution; they form the basis of the retrieval. The parameters IWC and r_e are the quantities we seek to retrieve, and values of Z are related to our measurements. We may also specify the columnar ice water content or ice water path (IWP),

$$\text{IWP} = \int_{z_{\text{base}}}^{z_{\text{top}}} \text{IWC}(z) dz. \quad (41)$$

The three parameters $N_T(z)$, $D_g(z)$, and $\sigma_{\log}(z)$ fully define the size distribution. Ice water content and effective radius may then be obtained through (36) and (37). Because the measured data are limited to a single radar reflectivity factor Z' for each radar resolution bin, we rely on *a priori* data to constrain the retrieval where the measurements cannot, allowing the retrieved solution to be consistent with the measurements without imposing fixed values of (e.g.) particle number concentration through the cloud column. The optimal estimation technique employed in this retrieval is described in section 3.2.

3.1.2 Algorithm refinements: correction for Lorenz-Mie effects

At frequencies of radars commonly used for cirrus cloud detection (35 or 94 GHz), the size parameter (the ratio between the diameter of the particle D and the radar wavelength λ) remains smaller than unity for crystal sizes up to 100 μm (and even larger for 35 GHz). Therefore, the Rayleigh approximation is almost always satisfied at these frequencies. However, because radar reflectivity in the Rayleigh regime is a function of the *sixth* power of the particle diameter, the error introduced by use of the Rayleigh approximation on the large crystals that violate the Rayleigh criterion may be significant, even if these coarser particles are few in number. To quantify this error, we performed Lorenz-Mie calculations and parameterized the ratio of the (exact) Lorenz-Mie radar reflectivity to the (approximate) Rayleigh reflectivity in terms of the size distribution parameters. Starting from the most general form of the radar equation, we have

$$\frac{P_r}{P_t} = \frac{\tilde{C}\lambda^2}{R^2} \int n(D) C_b(D) dD, \quad (42)$$

where \tilde{C} is the generalized radar constant and $C_b(D)$ is the *backscattering* coefficient. In the Rayleigh limit, $C_b(D)$ takes the form

$$C_b(D) = \frac{\pi^5}{\lambda^4} |K|^2 D^6, \quad (43)$$

where K is given by

$$K = \frac{m^2 - 1}{m^2 + 2}, \quad (44)$$

where m is the complex index of refraction of the particle material (water ice) at the radar frequency and ambient temperature. The dependence on the sixth power of the diameter in the radar reflectivity definition derives from (43).

The Lorenz-Mie theory provides an exact expression for C_b for homogeneous spheres that can be used instead of (43) to define an equivalent ‘‘Mie’’ radar reflectivity, Z_{Mie} . We computed Z_{Mie} using a code provided by Bohren and Huffman (1983) and plotted the ratio of Z_{Mie} and Z_{Ray} as a function of the distribution parameters D_g and σ_{\log} . At small particle sizes, the ratio is unity, indicating that the Rayleigh approximation is valid. For larger sizes, the two quantities begin to diverge, but the shape of the ratio function is well fitted by the following combination of Gaussian functions:

$$f_{\text{Mie}}(D_g, \sigma_{\log}) = \frac{Z_{\text{Mie}}}{Z_{\text{Ray}}} = A_0 \exp \left[-\frac{1}{2} \left(\frac{D_g}{A_1} \right)^2 \right] + A_2 \quad (45)$$

where

$$A_0 = a_{01} + a_{02} \exp \left[-\frac{1}{2} \left(\frac{\sigma_{\log} - 1}{a_{03}} \right)^2 \right] \quad (46)$$

$$A_1 = a_{11}(\sigma_{\log} - 1)^2 + a_{12} \quad (47)$$

$$A_2 = a_{21}(\sigma_{\log} - 1)^2 \quad (48)$$

where a_{01} , a_{02} , a_{03} , a_{11} , a_{12} , and a_{21} are specific coefficients of the fit. The expression f_{Mie} derived to account for the Lorenz-Mie effects has analytical properties and is differentiable, as is the radar forward model of (39). The new forward model can be written as

$$Z = Z_{\text{Ray}} f_{\text{Mie}}(D_g, \sigma_{\log}). \quad (49)$$

3.1.3 Further possible algorithm refinements: correction for density effects

Radar reflectivity is conventionally defined with respect to water Z_e , even when the radar target is known to be a volume of ice particles. To transform the ice quantities into equivalent radar reflectivity with respect to water, a constant correction factor defined as the ratio of K_{ice} and K is introduced, where these constants are proportional to the refractive index. In so doing, an implicit assumption is also made that the density of ice crystals is constant. The refractive index from porous ice particles such as large snow flakes/aggregates is generally considered to be some mixture of ice and air and is thus reduced in value from that of solid ice. Future versions of the retrieval will attempt to treat the effects of porosity by making K_{ice} a function of density. [Matrosov (1999) discusses this problem in great detail.] In the current version of the algorithm, no density correction is implemented. The equivalent reflectivity factor is thus written

$$Z_e = Z_{\text{Ray}} f_{\text{Mie}}(D_g, \sigma_{\log}) \tilde{K} \quad (50)$$

where $\tilde{K} = 0.232$ is a fixed correction factor (Stephens 1994).

3.1.4 Departures from the Lognormal Distribution

The retrieval assumes a lognormal distribution of ice particles, as given in (31). Departures from this distribution will degrade the accuracy of the retrieval. One source of departure from this analytic distribution is the presence of large particles within the cloud that may introduce a bimodality in the particle spectra (e.g., in thick anvil cirrus). Reflectivities greater than -15 dBZ are indicated in the output by setting a flag; but the algorithm is still run as normal, producing output values (unless the solution diverges). The flag serves as an indicator that the solution is likely unreliable due to a violation of the lognormal distribution assumption.

3.1.5 Mixed phase and multi-layered clouds

The ice water content retrieval algorithm assumes that the entire cloud column is composed of ice particles, except for bins having ECMWF-AUX temperatures warmer than 1°C , which are omitted from the retrieval. (The retrievals used in 2B-CWC-RO consider only one phase of water at a time.) Because we have no independent means of determining the particle phase in a given radar bin, a simple partition scheme is employed to create a composite ice/liquid profile, discarding the retrieved ice properties in portions of the profile deemed to consist purely of liquid. The partition scheme is described in section 4.

3.2 Retrieval Algorithm

The ice retrieval uses the same optimal estimation framework used by the liquid retrieval as described in section 2.2. The various input and output quantities are described here; see Austin et al. (200X) and Benedetti et al. (2003) for a more detailed description.

3.2.1 State and Measurement Vectors

The state vector \mathbf{x} is the vector of unknown cloud parameters to be retrieved. To ensure positivity of the retrieved quantities, the retrieval is formulated in logarithmic form for some of the unknowns following Fujita and Sataka (1997). For a cloud reflectivity profile consisting of p cloudy bins, the state vector will have $n = 3p$ elements:

$$\mathbf{x} = \begin{bmatrix} \log_{10} D_g(z_1) \\ \vdots \\ \log_{10} D_g(z_p) \\ \log_{10} N_T(z_1) \\ \vdots \\ \log_{10} N_T(z_p) \\ \sigma_{\log}(z_1) \\ \vdots \\ \sigma_{\log}(z_p) \end{bmatrix}, \quad (51)$$

where $D_g(z_i)$, $N_T(z_i)$, and $\sigma_{\log}(z_i)$ are the geometric mean diameter, number concentration, and distribution width parameter for height z_i (we shall often write these as D_{g_i} , etc.). Here z_1 is the height of the radar resolution bin at cloud base; z_p is at the top of the cloud profile. The units of D_g are mm and the units of N_T are m^{-3} ; σ_{\log} is dimensionless.

The measurement vector \mathbf{y} is identical to that used in the liquid retrieval, composed of $m = p$ elements for a cloud profile of p cloudy bins:

$$\mathbf{y} = \begin{bmatrix} Z'_{\text{dB}}(z_1) \\ \vdots \\ Z'_{\text{dB}}(z_p) \end{bmatrix}, \quad (52)$$

where $Z'_{\text{dB}}(z_i)$ is the measured radar reflectivity for height z_i (often written as Z'_{dB_i}). Reflectivity is specified in units of $\text{mm}^6 \text{m}^{-3}$. To reduce the large dynamic range of the reflectivity variable and to make the model more linear, Z has been converted to a logarithmic variable Z_{dB} by the transform $Z_{\text{dB}} = 10 \log Z$, where Z_{dB} has units of dBZ and \log indicates the base 10 logarithm. Because ice particle attenuation is small (compared to attenuation by liquid particles), ice particle attenuation effects are neglected in this version of 2B-CWC-RO.

The measurement error covariance matrix \mathbf{S}_ϵ gives a measure of the uncertainties in the measurement vector and of correlations between the errors of the individual elements. It is identical to that used in the liquid retrieval (21).

3.2.2 Forward Model and Parameters

The forward model $\mathbf{F}(\mathbf{x})$ relates the state vector \mathbf{x} to the measurement vector \mathbf{y} . \mathbf{F} therefore has the same dimension as \mathbf{y} :

$$\mathbf{F}(\mathbf{x}) = \begin{bmatrix} Z'_{\text{dB}_{\text{FM}}}(z_1) \\ \vdots \\ Z'_{\text{dB}_{\text{FM}}}(z_p) \end{bmatrix}, \quad (53)$$

where the individual elements are given by the following expression:

$$Z'_{\text{dB}_{\text{FM}}}(z_i) = 10 \log [N_T D_g^6 \exp(18\sigma_{\log}^2) f_{\text{Mie}}(D_g, \sigma_{\log}) \tilde{K}], \quad i = 1, \dots, p \quad (54)$$

where the symbol Δz represents the spacing between radar range bins. The subscript FM is a reminder that these quantities are calculated from elements of \mathbf{x} according to the forward model equation (54), as opposed to the elements of the \mathbf{y} vector, which are measured quantities.

3.2.3 A Priori Data and Covariance

A priori data values for the ice retrieval are selected in two ways. Values of D_g and σ_{\log} are determined using temperature-based parameterizations constructed from collections of ice particle size distribution measurements from aircraft flights during recent field campaigns. The values therefore vary through the cloud profile according to the temperature indicated by the CloudSat ECMWF-AUX data product. A different procedure was used to set the *a priori* N_T value. Rather than using a temperature-based

value for this parameter, it was recognized that reflectivity values measured by CloudSat are sometimes very different from those predicted by the *a priori* database, even after taking temperature into account. In these cases, the number concentration parameter seemed the logical parameter to account for most of the difference. It was therefore deemed necessary to find a way to obtain a value of N_T that would be “closer” in state space to the set of values consistent with a given measurement. This was accomplished by combining (32), (39), and (50) and solving for N_T . The value of IWC was determined independently from Z_e using a Z -IWC relation from Liu and Illingworth (2000). Values of N_T were obtained for each cloudy bin and then averaged through the profile to obtain a single profile value of N_{Ta} , which was then used in the retrieval process. Uncertainties in all three parameters were then calculated using the values obtained from the aircraft measurement database.

The *a priori* vector \mathbf{x}_a for the ice retrieval is specified as follows:

$$\mathbf{x}_a = \begin{bmatrix} \log_{10} D_{ga}(z_1) \\ \vdots \\ \log_{10} D_{ga}(z_p) \\ \log_{10} N_{Ta}(z_1) \\ \vdots \\ \log_{10} N_{Ta}(z_p) \\ \sigma_{\log_a}(z_1) \\ \vdots \\ \sigma_{\log_a}(z_p) \end{bmatrix}. \quad (55)$$

We also specify an *a priori* error covariance matrix \mathbf{S}_a :

$$\mathbf{S}_a = \begin{bmatrix} \sigma_{\log_{10} D_{ga1}}^2 & 0 & \cdots & 0 & \cdots & 0 & 0 & \cdots & 0 \\ 0 & \ddots & 0 & \vdots & \vdots & \vdots & \vdots & \vdots & \vdots \\ \vdots & 0 & \sigma_{\log_{10} D_{gap}}^2 & 0 & \cdots & 0 & 0 & \cdots & 0 \\ 0 & \cdots & 0 & \sigma_{\log_{10} N_{Ta1}}^2 & 0 & \vdots & \vdots & \vdots & \vdots \\ \vdots & \cdots & \vdots & 0 & \ddots & 0 & \vdots & \vdots & \vdots \\ 0 & \cdots & 0 & \cdots & 0 & \sigma_{\log_{10} N_{TAp}}^2 & 0 & \vdots & \vdots \\ 0 & \cdots & 0 & \cdots & \cdots & 0 & \sigma_{\sigma_{\log_a1}}^2 & 0 & \vdots \\ \vdots & \cdots & \vdots & \cdots & \cdots & \cdots & 0 & \ddots & 0 \\ 0 & \cdots & 0 & \cdots & \cdots & \cdots & \cdots & 0 & \sigma_{\sigma_{\log_ap}}^2 \end{bmatrix}. \quad (56)$$

3.2.4 Convergence and Quality Control

Convergence criteria for the ice retrieval are identical to those used for the liquid retrieval (see section 2.2.4). The goodness-of-fit statistic is likewise identical.

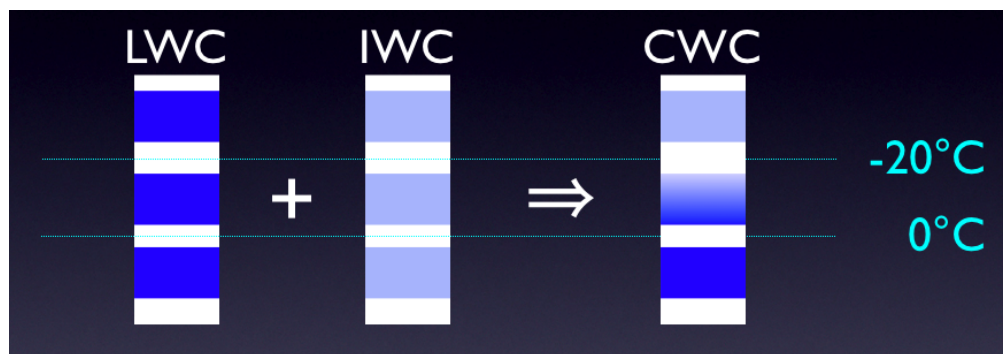


Figure 1: The CWC composite profile is built by combining the retrieved ice and liquid water profiles, according to temperature.

4 Algorithm Theoretical Basis—Cloud Water Content

The original list of CloudSat standard data products included separate products for liquid water content and ice water content. Because there was no independent means of determining the cloud phase in any given radar resolution bin, the plan was to run the liquid and ice retrievals separately on the entire radar profile, resulting in a set of liquid microphysical parameters for each cloudy bin and a corresponding set of ice microphysical parameters for each cloudy bin. The user would then select which answer would be more appropriate or combine the two in some way. No attempt would be made to partition the measured reflectivity between the liquid and ice phases—each solution would assume the entire radar signal was due to a single phase of water.

As the retrievals were further developed and the time approached for the first post-launch data releases, it became clear that this approach would be overly confusing and would likely result in “double-counting” of the cloud water content: users interpreting each cloudy bin as containing *both* liquid and ice water content. To avoid this confusion, a new combined cloud water content product and algorithm were developed. In the new algorithm, the liquid and ice retrievals are run separately on the entire radar profile (as before), but the two resultant profiles are then combined into a composite profile using a simple scheme based on temperature. In this scheme, the portion of the profile colder than -20°C is deemed pure ice, so the ice retrieval solution applies there. Similarly, the portion of the profile warmer than 0°C is considered pure liquid, so the liquid solution applies there. In between these temperatures, the ice and liquid solutions are scaled linearly with temperature (by adjusting the ice and liquid particle number concentrations) to obtain a profile that smoothly transitions from all ice at -20°C to all liquid at 0°C while matching the radar measurements over the whole range.

This scheme gives a very basic partition of the radar measurements into ice and liquid phases. (More sophisticated retrievals for heterogeneous cloud columns are planned for future versions of this product.) The product also contains a 16-bit status variable; individual bits in this variable indicate error conditions in the ice and liquid retrievals and other associated conditions such as large values of the fit parameters or possible precipitation. It is important to note that the partition algorithm is applied separately to the ice and liquid phases regardless of whether both retrievals were successful. For example, if the liquid retrieval fails to converge, the ice water content will still be scaled such that

it goes to zero as the temperature increases to 0°C—there is no attempt to map all the reflectivity to the ice phase to compensate for the failure of the liquid retrieval.

The 2B-CWC-RO data product files contain both the composite profiles (which most users will want to use) and the single-phase retrieval profiles (which may be of interest to some investigators). The output data from the liquid cloud retrieval (which interprets all cloud as liquid from the surface to the stratosphere) is found in fields with names starting with LO_RO_ (for “liquid-only” and “radar-only”). Corresponding outputs from the ice cloud retrieval have names starting with IO_RO_. The fields representing the combination of these into composite profiles have names beginning with RO_liq_ and RO_ice_. Consult the 2B-CWC-RO Interface Control Document for detailed descriptions of the fields contained in the 2B-CWC-RO HDF files.

5 Algorithm Inputs

5.1 CloudSat

5.1.1 CloudSat 2B-GEOPROF Data

The CloudSat 2B-GEOPROF product is the principal input for 2B-CWC-RO. The retrieval uses the radar reflectivity, the cloud mask, and the gaseous attenuation values from this product. For cases where this input is missing, 2B-CWC-RO will have no output.

5.1.2 CloudSat 2B-CLDCLASS Data

Various bits in cloud scenario field in the 2B-CLDCLASS product are used to detect cloud type and to screen problematic profiles. Future versions of the retrievals may use the indicated cloud type, surface type, and other flags to refine the retrieval algorithm, for example by selecting different *a priori* values according to cloud type.

5.2 Ancillary (Non-CloudSat)

5.2.1 CloudSat ECMWF-AUX Data

The retrieval uses temperature information from the CloudSat ECMWF-AUX product, which takes model output from ECMWF and interpolates the variables to the CloudSat data grid. Temperature information is used to assign *a priori* values in the ice cloud retrieval and also to guide the combination of the ice and liquid information into composite profiles.

6 Algorithm Summary

The algorithm is implemented in Fortran 90. The following is a pseudocode description of the algorithm implementation:

```

start 2B-LWC-RO
get orbit of 2B-GEOPROF data (CPR cloud mask, radar reflectivity)
get orbit of 2B-CLDCLASS data (cloud scenario)
for-each 2B-GEOPROF vertical profile
    convert bit flags to integer values
    determine if LWC retrieval will be run (known & valid cloud scenario, cloud present,  $Z$  physical)
    if running LWC retrieval
        determine size of state vector
        assign a priori  $r_g$ ,  $N_T$ , and  $\sigma_{\log}$  values and uncertainties
        set  $y$  vector (2B-GEOPROF) using condensed profile retaining cloudy bins only
        set  $S_a$ ,  $S_a^{-1}$ ,  $S_\epsilon$  matrices
        repeat
            calculate  $K$ ,  $S_y$ ,  $D_y$  matrices
            calculate  $F$  (forward-model) vector
            calculate  $S_y^{-1}$ ,  $S_x^{-1}$ ,  $S_x$  matrices
            calculate new state vector  $\hat{x}$ 
            if  $\hat{x}$  goes negative, reject
            calculate  $\Delta\hat{x}$ , convergence test
            if more than 15 iterations, reject
        end-repeat until convergetest  $< 0.01n$ 
        calculate  $r_e$ , LWC, LWP
        calculate  $\chi^2$  and  $A$ 
        calculate retrieval uncertainties
        calculate output percent uncertainties
        load output variables
    else
        ; RO LWC retrieval not run
        load output variables with error values and set status flags
    end-if (running LWC retrieval)
end-for (loop over profiles)

```

```

calculate metadata statistics
end 2B-LWC-RO

start 2B-IWC-RO

get orbit of 2B-GEOPROF data (CPR cloud mask, radar reflectivity)
get orbit of 2B-CLDCLASS data (cloud scenario)

for-each 2B-GEOPROF vertical profile

    convert bit flags to integer values
    determine if IWC retrieval will be run (known & valid cloud scenario, cloud present,  $Z$  physical)
    if running IWC retrieval

        determine size of state vector
        assign a priori  $D_g$ ,  $N_T$ , and  $\sigma_{\log}$  values and uncertainties
        set  $y$  vector (2B-GEOPROF) using condensed profile retaining cloudy bins only
        set  $S_a$ ,  $S_a^{-1}$ ,  $S_\epsilon$  matrices
        repeat

            calculate  $K$ ,  $S_y$ ,  $D_y$  matrices
            calculate  $F$  (forward-model) vector
            calculate  $S_y^{-1}$ ,  $S_x^{-1}$ ,  $S_x$  matrices
            calculate new state vector  $\hat{x}$ 
            calculate  $\Delta\hat{x}$ , convergence test
            if more than 15 iterations, reject
        end-repeat until convergetest < 0.01n
        calculate  $r_e$ , IWC, IWP
        calculate  $\chi^2$  and  $A$ 
        calculate retrieval uncertainties
        calculate output percent uncertainties
        load output variables

    else

        ; RO IWC retrieval not run
        load output variables with error values and set status flags

    end-if (running IWC retrieval)

end-for (loop over profiles)

calculate metadata statistics

end 2B-IWC-RO

```

start 2B-CWC-RO
get orbit of 2B-GEOPROF data
get orbit of 2B-LWC-RO data
get orbit of 2B-IWC-RO data
get orbit of ECMWF-AUX data
calculate ice phase fraction from temperature for all cloudy bins
calculate liquid phase fraction from temperature for all cloudy bins
map liquid properties into composite profiles, scaling bins by liquid phase fraction
map ice properties into composite profiles, scaling bins by ice phase fraction
calculate revised ice and liquid water path from composite profiles
copy error fill values into composite profiles
add error codes for other error conditions
set flags in status variable
write metadata statistics to text file
end 2B-CWC-RO

7 Data Product Output Format

The 2B-CWC-RO data product includes swath data and metadata in an HDF-EOS formatted file. Users are directed to the 2B-CWC-RO Interface Control Document for a full description of the data and metadata fields contained in the product. Scale factors used in converting file values into science data values are included in the file as HDF variable attributes. Users are encouraged to read scale factors directly from the file (rather than from written documentation), because the scale factors may change.

8 Changes since version 5.0

The following list summarizes the changes since version 5.0 of the 2B-CWC-RO product (which was released in release R03):

- Liquid Water Content
 - Number concentration and width parameter now allowed to vary with altitude
 - Change scale factor of some HDF variables
- Ice Water Content
 - Change from modified gamma to lognormal size distribution
 - Number concentration and width parameter now allowed to vary with altitude
 - Change scale factor of some HDF variables
 - Change to temperature-based selection of *a priori* values
 - Omit cloudy bins warmer than +1°C (because no *a priori* values apply)
 - Change parameterization of f_{Mie} ratio
- Cloud Water Content
 - Report profiles of all three size distribution parameters for both ice and liquid
 - Ice retrieval now uses lognormal distribution
 - Change scale factor of some HDF variables

References

- [1] Austin, R. T., and G. L. Stephens, Retrieval of stratus cloud microphysical parameters using millimeter-wave radar and visible optical depth in preparation for CloudSat, 1. Algorithm formulation, *J. Geophys. Res.*, *106*, 28 233–28 242, 2001.
- [2] Austin, R. T., and G. L. Stephens, Improved retrieval of stratus cloud microphysical parameters using millimeter-wave radar and visible optical depth, 1. Algorithm and synthetic analysis, in preparation, 200X.
- [3] Austin, R. T., et al., Improved retrieval of cirrus cloud microphysical parameters, in preparation, 200X.
- [4] Benedetti, A., G. L. Stephens, and J. M. Haynes, Ice cloud microphysical parameters using millimeter radar and visible optical depth using an estimation theory approach, *J. Geophys. Res.*, *108*, 4335, doi:10.1029/2002JD002693, 2003.
- [5] Bohren, C., and D. R. Huffman, *Absorption and scattering of light by small particles*, John Wiley & Sons, Inc., New York, 1983.
- [6] Fujita, M., and M. Satake, Rainfall rate profiling with attenuating-frequency radar using nonlinear LMS technique under a constraint on path-integrated rainfall rate, *Int. J. Remote Sensing*, *18*, 1137–1147, 1997.
- [7] Liu, C.-L., and A. J. Illingworth, Toward more accurate retrievals of ice water content from radar measurements of clouds, *J. Appl. Meteor.*, *39*, 1130–1146, 2000.
- [8] Marks, C. J., and C. D. Rodgers, A retrieval method for atmospheric composition from limb emission measurements, *J. Geophys. Res.*, *98*, 14,939–14,953, 1993.
- [9] Matrosov, S. Y., Retrievals of vertical profiles of ice cloud microphysics from radar and IR measurements using tuned regressions between reflectivity and cloud parameters, *J. Geophys. Res.*, *104*, 16 741–16 753, 1999.
- [10] Miles, N. L., J. Verlinde, and E. E. Clothiaux, Cloud droplet size distributions in low-level stratiform clouds, *J. Atmos. Sci.*, *57*, 295–311, 2000.
- [11] Rodgers, C. D., Retrieval of atmospheric temperature and composition from remote measurements of thermal radiation, *Rev. Geophys.*, *14*, 609–624, 1976.
- [12] Rodgers, C. D., Characterization and error analysis of profiles retrieved from remote sounding measurements, *J. Geophys. Res.*, *95*, 5587–5595, 1990.
- [13] Rodgers, C. D., *Inverse Methods for Atmospheric Sounding: Theory and Practice*, World Scientific Publishing, Singapore, 2000.
- [14] Stephens, G. L., *Remote sensing of the lower atmosphere*, Oxford University Press, Oxford, 1994.